Journal of Solid Mechanics Vol. 14, No. 4 (2022) pp. 430-446
DOI: 10.22034/jsm.2020.1895149.1558

Research Paper

Magneto-Rheological Response in Vibration of Intelligent Sandwich Plate with Velocity Feedback Control

A. Mihankhah[1], Z. Khoddami Maraghi [2], A. Ghorbanpour Arani [1,3 *], S. Niknejad [1]

[1]*Faculty of Mechanical Engineering, University of Kashan, Kashan, Iran*
[2]*Faculty of Engineering, Mahallat Institute of Higher Education, Mahallat, Iran*
[3]*Institute of Nanoscience and Nanotechnology, University of Kashan, Kashan, Iran*

Received 5 July 2022; accepted 8 September 2022

ABSTRACT

This study deals with the free vibration of the sandwich plate made of two smart magnetostrictive face sheets and an electro-rheological fluid core. Electro-rheological fluids are polymer-based material that changes its viscosity under the applied electric field. A feedback control system follows the magnetization effect on the vibration characteristics of the sandwich plate when subjected to the magnetic field. It is assumed that there is no slip between layers, so the stress-strain relations of each layer are separately considered. Energy method is utilized in order to derive the five coupled equations of motion. These equations are solved by differential quadrature method (DQM). Results of this study show the rheology response of fluid in presence of electric field where the core gets hard and the dimensionless frequency increases. Also, the significant effect of thickness and aspect ratios and velocity feedback gain are discussed in detail. Such intelligent structures can replace in many of the systems used in automotive, aerospace and building industries as the detector, warning, and vibration absorber etc.

Keywords : Sandwich structure; Feedback control system; Electro-rheological fluid; Magnetostrictive sheets, Free vibration.

1 INTRODUCTION

THIS paper studied a sandwich structure containing new smart materials. The core of sandwich is Electro-rheological (ER) fluid and face sheets are magnetostrictive materials (MsM). Therefore, this section introduced two intelligent materials and related papers about them. Smart-ER fluids are designed and manufactured to function as a non-toxic, high-strength, adaptive engineering material. ER fluids cause significant inverse changes in material characteristics when exposed to electrical potential differences. The most marked change in them when applied to the electric field is the change in the complex shear modulus of matter. This dual behavior makes ER fluids useful in many semi-active vibration control systems and suspension systems where variable damper is used [1]. Mikhasev et al. [2] modeled the physical properties of the smart face sheets of sandwich shell. They introduced the magnetic field as some founctions and investigated laminated cylindrical shells with magnetorheological elastomers (MREs)

*Corresponding author. Tel.: +98 31 55912450; Fax: +98 31 55912424.
E-mail address: aghorban@kashanu.ac.ir (A.Ghorbanpour Arani)

as core and elastic layers. They analyzed the effect of intensity of applied magnetic field on natural frequencies and damping decrement. Arumugam et al. [3] investigated the effect of the MR fluid on the instability of composite sandwich plate. In this work, the in-plane load was periodically applied to the sandwich plate and rotate with constant velocity. They showed that the buckling load increases with increase in magnetic field. Malekzadeh Fard et al. [4] were utilized the MR fluid as face sheets of cylindrical sandwich panel to study the vibration behavior and critical buckling load. They investigated the effect magnetorheological fluid, geometrical parameters on natural vibration frequency and loss factor. Also, in the present paper ABAQUS software was used to simulate the cylindrical sandwich panel. Sainsbury and Zhang [5] modeled the sandwich beam with damping using a new finite element. They are provided displacement continuity condition between the damping and elastic layers. With this method, only a limited number of elements were needed to accurately investigate the frequency response of the structure. The dynamic stability problems of a sandwich plate with top and bottom elastic layers and an ER fluid core were investigated by Yeh and Chen [6] when applying an axial dynamic force. Instability analysis was performed using finite element method and harmonic equilibrium method. They studied the change of loss factors and natural frequencies, in addition the static cylindrical loads on the stability of sandwich plate. Lu and Meng [7] investigated the dynamic behavior of a ER sandwich plate. They performed a laser holographic interference test and, with the help of laboratory tests, provided a way to determine the natural frequencies, the loss factor, and the composite structure shapes in various electrical loads. They also developed a discrete dynamic model based on the special properties of the ER fluid. Yeh and Chen [8] considered an orthotropic sandwich plate with an ER fluid core and investigated its dynamic stability characteristics by calculating the main plate instability zones using the finite element method and the harmonic equilibrium method. Their results showed the effect of geometrical parameters, mechanical properties, and electric field on orthotropic sandwich plate instability. Narayana and Ganesan [9] were compaired the effect of critical damping in viscoelastic materials and ER fluid as a core of composite sandwich skew plates. They calculated the frequency and loss factor by considering the boundary conditions, electric field, core to face sheet thickness ratios. Dynamic analysis of a sandwich plate with an orthotropic face sheets and ER fluid core was analyzed by Yeh and Chen [10] using finite element method. Their results showed the effect of modal damping, loss factors, rheological property, electric field and thickness ratio on natural frequency. Yeh [11] analyzed the vibration and viscoelastic behavior of the annular sandwich plate with ER fluid core. He derived the equations of motion using Rayleigh-Ritz method and calculated the natural frequencies and loss factors of sandwich plate. The dynamic behavior of the sandwich annular plate showed the damping of plate is more effective in the presence of the electric field. Allahverdizadeh et al. [12] were analyzed dynamic behavior of adaptive sandwich beams with ER fluid middle layer and functionally graded materials constraining layers. Finite element formulation was developed and validated for functionally graded ER beams. They considered a complex shear modulus for modeling the viscoelastic core and used experimental and computational analysis. Tabassian and Rezaeepazhand [13] studied dynamic stability of electro-rheological (ER) sandwich beams resting on Winkler sybstrate exposed to the harmonic axial forces. They investigated the influences of various parameters such as lenght-to thickness ration, static load, applied voltage, foundation stiffness and ER properties layer on critical dynamic loads and stability regions of the beam.Hoseinzadeh and Rezaeepazhand [14] investigated the effects of external ER dampers on the dynamic response of composite laminated plates. They considered the Bingham plastic model to simulate the properties of ER fluid and obtained the finite element formulation for this structure according to the first order shear deformation theory (FSDT). Free vibration analysis of a sandwich rectangular plate with a constrained layer and an ER fluid core was carried out by Soleymani et al. [15]. Using Navier solution method, they obtained natural frequencies and loss factors for different intensity values of electric field. Eshaghi et al. [16] presented a comprehensive review of researches on applications of magnetorheological (MR)/ER fluids for realizing active and semi-active vibration suppression in sandwich structures. Hasheminejad and Aghayi Motaaleghi [17] analyzed the supersonic flutter control of ER sandwich curved panels. They utilized Kirchhoff–Love thin shell theory, the first order Kelvin–Voigt viscoelastic material model, and the linear quasi-steady Krumhaar's modified supersonic piston theory to formulate this problem. Asgari and Kouchakzadeh [18] studied the aeroelastic characteristics of MR fluid sandwich beams subjected to the supersonic airflow. They discussed about the influences of applied magnetic field, constraining layer thickness and core layer thickness on the critical aerodynamic pressure. Analytical and experimental free vibration analysis of sandwich circular plate made of MR fluid core and Polyethylene Terephthalate Glycol facesheets were investigated by Eshaghi et al. [19]. They used an analytical model to derive the equations of motion according to the classical plate theory and Ritz method. Ghorbanpour Arani et al. [20] considered free vibration behavior of sandwich plate with ER fluid core and nanocomposite facesheets which is rested on Winkler-Pasternak substrate. They calculated the material properties of ER core and nanocomposite facesheets based on Don and Yalcintas models, and Eshelby-Mori-Tanaka approach, respectively. MsMs are a type of intelligent material that react against the magnetic potential difference. These materials are capable of producing a

magnetic field even when deformed. Due to the engineering application of these materials, extensive research has been conducted in recent decades on the different types of these materials. The transient response of composite plates with smart lamina was studied by Lee et al. [21] using a unified plate theory. Smart layers (Terfenol-D) are used to control the vibration suppression by a simple velocity feedback gain. They studied the vibration suppression of plate under the effect of smart layer position and thickness and material properties. Hong [22] investigated the transient response of three-layer laminated magnetostrictive plate using the generalized differential quadrature (GDQ) method with a few grid points. He also controlled the vibration suppression of a smart laminated plate with the help of velocity feedback control gain.Vibrational behaviors of the magnetostrictive plate (MsP) subjected to the follower force and magnetic field were studied by Ghorbanpour Arani and Khoddami Maraghi [23]. They used the velocity feedback gain parameter to evaluate the effect of the magnetic field generated by the coil. Their findings showed the effects of geometric parameters, follower force and velocity feedback gain on the frequency of MsP. Ghorbanpour Arani et al. [24] studied free vibration of five layers' micro-plate made of piezomagnetic, piezoelectric and composite materials. They used First-order shear deformation theory to derive the seven coupled equations of motion and solved by DQM. Their results showed the effect of geometric parameters and electro–magneto-mechanical loadings on the vibration behavior of sandwich plate.

Free vibration of the sandwich plate composed of upper and lower magnetostrictive layers and ER fluid core is a new topic that cannot be found in the literature. A rheological response of ER fluid is simulated by Don and Yalcintas models where the complex shear modulus is introduced based on Bingham plastic model. For ER materials, this property is dependent on the external electric field. MsM is one of the substances in control systems because of its dual nature. Stress changes due to external magnetic field have created magneto-mechanical coupling in these materials and such a property can be used in systems stability. The results of this study investigated the effect of geometric parameters, velocity feedback gain parameters and electric field on vibrational behavior of the sandwich plate that can be useful to in many industries. This structure is used to enhance the stability of mechanical systems.

2 STRUCTURAL DEFINITION

Fig.1 illustrates a sandwich plate with three layers, in which geometrical parameters of length a, width and thickness $2h_m + h_c$ are also indicated.

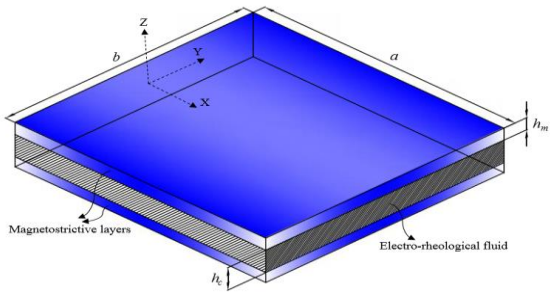

Fig.1
A schematic diagram of a sandwich plate.

As shown in Fig. 1 the structure that studied in this paper is composed three layers:

1. Central layer filled by Electro-rheological fluid,
2. Top and bottom layers (face sheets) made of MsM.

The strain and kinetic energy of each layers are separately written and the total energy equation which includes the energy of ER core and Ms face sheet are obtained using the Hamilton's principle.

3 CONSTITUTIVE EQUATIONS

Electrical materials are suspensions of dielectric particles in non-polar fluids whose rheological response changes dramatically under the applied electric field [25]. The Electro-rheological fluids are the materials with polymer base and its viscosity change with applied electric field that would be impressed their dimensions. Applied electric field

transforms liquid to a solid like gel. For example, these materials are used in automotive shock absorbers in new vehicles so that the height of vehicle can be adjusted by changing the flow. It is assumed that the ER fluid under certain voltage is isotropic. Eq. (4) illustrates the stress-strain relation for isotropic material [26]:

$$\begin{bmatrix}\sigma_{xx}\\ \sigma_{yy}\\ \sigma_{xy}\\ \sigma_{xz}\\ \sigma_{yz}\end{bmatrix}=\begin{bmatrix}Q_{11} & Q_{12} & 0 & 0 & 0\\ Q_{21} & Q_{22} & 0 & 0 & 0\\ 0 & 0 & Q_{44} & 0 & 0\\ 0 & 0 & 0 & Q_{55} & 0\\ 0 & 0 & 0 & 0 & Q_{66}\end{bmatrix}\begin{bmatrix}\varepsilon_{xx}\\ \varepsilon_{yy}\\ \varepsilon_{xy}\\ \varepsilon_{xz}\\ \varepsilon_{yz}\end{bmatrix} \tag{1}$$

where σ_{ij} and ε_{ij} are normal and shear stresses and the stiffness constants are yield as:

$$Q_{11}=Q_{22}=\frac{E}{(1-\upsilon^2)},\quad Q_{12}=Q_{13}=\frac{E\upsilon}{(1-\upsilon^2)},\quad Q_{44}=Q_{55}=\frac{E}{2(1+\upsilon)},\quad Q_{66}=\frac{E}{2(1+\upsilon)} \tag{2}$$

In which E and υ are Young modulus and Poisson's ratio respectively. Eqs. (1) and (2) are valid for ER core and magnetostrictive face sheets. In this regard to obtaining the elastic elastic model is used to modeling Electric fluids in the pre-yield regime and Bingham plastic model for post-yield regime [27]. Properties of the central core and magnetostrictive face sheet, are presented in the next sections.

3.1 ER fluid

Electric fluids behave like Newtonian fluids when the electric field is not applied to them. But in the presence of an electric field, their nature is changed and behaves like a solid gel. The yield point is the decisive point in the rheological response of these materials. For the ER core, it is assumed that:

1. Isotropic.
2. ER core acts as a Bingham plastic material.
3. Normal stress in the ER core is neglected because the Young's modulus of MR fluids is very low compared to MS face sheets,
4. There is no slip between layers.
5. Transverse displacement is the same in all points on a cross-section.

According to the above kinetic, the displacement filed of Ms face sheets can be expressed [28]:

$$\begin{aligned}&u_i(x,y,z,t)=u_i(x,y,z)-z_i\frac{\partial w}{\partial x},\\ &v_i(x,y,z,t)=v_i(x,y,z)-z_i\frac{\partial w}{\partial x},\\ &w_i(x,y,z,t)=w(x,y),\end{aligned} \tag{3}$$

According to the mentioned assumptions, as the Fig. 2 implies, strain-displacement relations for ER fluid as follows [29]:

$$\begin{aligned}&\varepsilon_{xxi}=\frac{\partial u_i}{\partial x}-z_i\frac{\partial^2 w}{\partial x^2},\\ &\varepsilon_{yyi}=\frac{\partial v_i}{\partial y}-z_i\frac{\partial^2 w}{\partial y^2},\\ &\gamma_{xyi}=\frac{\partial u_i}{\partial y}+\frac{\partial v_i}{\partial x}-2z_i\frac{\partial^2 w}{\partial x\,\partial y},\ i=1,3\end{aligned} \tag{4}$$

(u_i, v_i) are displacements of the middle plane in (x, y) direction. With regard to strain-displacement relations in ER core, shear deformation $(\gamma_{xz2}, \gamma_{yz2})$ is written as follows [30,31]:

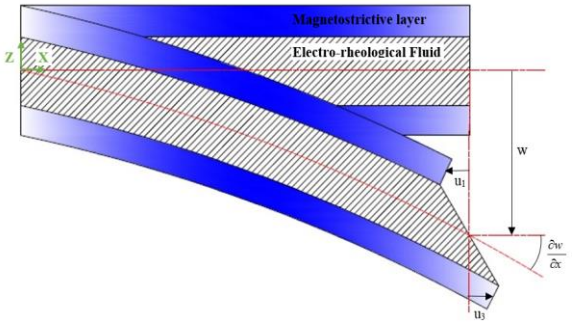

Fig.2
Adjustment layer after deformation.

$$\gamma_{xz2} = \frac{\partial w}{\partial x} + \frac{\partial u_2}{\partial z}, \quad \gamma_{yz2} = \frac{\partial w}{\partial y} + \frac{\partial v_2}{\partial z} \tag{5}$$

w is displacements of the middle plane in $z-$direction. The geometry of deformation leads to Eq. (6). In this relationship, $\left(\frac{\partial u_2}{\partial z}, \frac{\partial v_2}{\partial z}\right)$ are the total shear deformations due to rotation $\left(\Delta u_{rotation}\right)$ and elongation $\left(\Delta u_{elongation}\right)$ and calculate according to the following equations [25]:

$$\frac{\partial u_2}{\partial z} = \frac{\Delta u_{rotation} + \Delta u_{elongation}}{h_2} = \frac{1}{h_2}\left(\frac{h_1}{2} + \frac{h_3}{2}\right)\frac{\partial w}{\partial x} + \frac{u_1 - u_3}{h_2} = \frac{h_1 + h_3}{2h_2}\frac{\partial w}{\partial x} + \frac{u_1 - u_3}{h_2},$$
$$\frac{\partial v_2}{\partial z} = \frac{\Delta v_{rotation} + \Delta v_{elongation}}{h_2} = \frac{1}{h_2}\left(\frac{h_1}{2} + \frac{h_3}{2}\right)\frac{\partial w}{\partial y} + \frac{v_1 - v_3}{h_2} = \frac{h_1 + h_3}{2h_2}\frac{\partial w}{\partial y} + \frac{v_1 - v_3}{h_2}, \tag{6}$$

In which h_m for upper and lower magnetostrictive layers is called h_1 and h_2 respectively. In the other hands, the compatibility relations are written as follows [25,29]:

$$\gamma_{xz2} = \frac{d}{h_2}\frac{\partial w}{\partial x} + \frac{u_1 - u_3}{h_2}, \quad \gamma_{yz2} = \frac{d}{h_2}\frac{\partial w}{\partial y} + \frac{v_1 - v_3}{h_2}, \tag{7}$$

where $d = h_1/2 + h_2 + h_3/2.$

3.2 Magnetostriction effect

Magnetostrictive materials possess undergo dimensional changes under applied magnetic fields due to anisotropy in their atomic structure [13]. To investigate the effect of the magnetic field on MsM, the magneto-mechanical coupling based on the experimental results appears as follows [32]:

$$\begin{bmatrix} \sigma^m_{xx} \\ \sigma^m_{yy} \\ \sigma^m_{xy} \end{bmatrix} = \begin{bmatrix} \bar{C}_{11} & \bar{C}_{12} & 0 \\ \bar{C}_{21} & \bar{C}_{22} & 0 \\ 0 & 0 & \bar{C}_{44} \end{bmatrix} - \begin{bmatrix} 0 & 0 & e_{31} \\ 0 & 0 & e_{32} \\ 0 & 0 & e_{34} \end{bmatrix} \begin{bmatrix} 0 \\ 0 \\ H_z \end{bmatrix}. \tag{8}$$

Index m refers to magnetic stress ($\bar{C}_{ij}$ for magnetostrictive face sheets instead $\bar{Q}_{ij}$ for ER core). H_z is the magnetic field intensity and e_{ij} is the magnetostrictive coupling modules which can be expressed as the magnetic field of a coil [22,32,33].

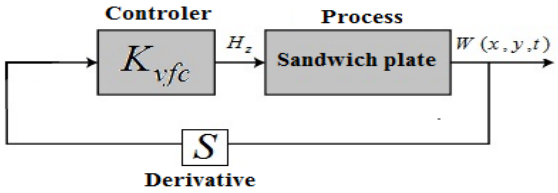

Fig.3
Control loop.

$$H_z = K_{vfc}\frac{\partial w_0(x,y,t)}{\partial t} \tag{9}$$

where K_{vfc} is introduced as velocity feedback gain. Fig. 3 displays a simple control loop that used in this sandwich for magnetostrictive layers. As it been defined in Eq. (9), the derivative operator is applied on $w_0(x,y,t)$. Also e_{31}, e_{32}, e_{34} are determined as follow [22,23]:

$$\begin{aligned} e_{31} &= \bar{e}_{31}\cos^2\theta + \bar{e}_{32}\sin^2\theta, \\ e_{32} &= \bar{e}_{31}\sin^2\theta + \bar{e}_{32}\cos^2\theta, \\ e_{34} &= (\bar{e}_{31} - \bar{e}_{32})\sin\theta\sin\theta. \end{aligned} \tag{10}$$

where θ represents the direction of magnetic anisotropy and the values of $\bar{e}_{31}, \bar{e}_{32}, \bar{e}_{34}$ are reported in Table 1.

4 ENERGY METHOD IN SANDWICH PLATE

4.1 Strain energy

In this section, the energy method is used as a comprehensive method in deriving the equations of motion. Strain energy of the rectangular sandwich plate is calculated as [34]:

$$\begin{aligned} U &= \frac{1}{2}\int_V \left(\sigma_{xx}\varepsilon_{xx} + \sigma_{yy}\varepsilon_{yy} + \sigma_{xy}\gamma_{xy} + \sigma_{xz}\gamma_{xz} + \sigma_{yz}\gamma_{yz}\right)dx\,dy\,dz \\ U_{sandwich} &= U_{ERcore} + U^{Bottom}_{Face\,sheet} + U^{Top}_{Face\,sheet} \\ U^{Bottom}_{Face\,sheet} &= \frac{1}{2}\int_{-h_m}^{-\frac{h_c}{2}}\int_0^b\int_0^a \left(\sigma^m_{xx}\varepsilon_{xx} + \sigma^m_{yy}\varepsilon_{yy} + \sigma^m_{xy}\gamma_{xy}\right)_{lowerSheet} dx\,dy\,dz \\ U^{Top}_{Face\,sheet} &= \frac{1}{2}\int_{\frac{h_c}{2}}^{\frac{h_c}{2}+h_m}\int_0^b\int_0^a \left(\sigma^m_{xx}\varepsilon_{xx} + \sigma^m_{yy}\varepsilon_{yy} + \sigma^m_{xy}\gamma_{xy}\right)_{upperSheet} dx\,dy\,dz \\ U_{ER\,core} &= \int_V G_2\left(\gamma^2_{xz\,2} + \gamma^2_{yz\,2}\right)dV \end{aligned} \tag{11}$$

4.2 Kinetic energy

The kinetic energy of sandwich plate is composed of three parts:

1. Kinetic energy corresponding with inplane displacement:

$$K_{Face\ sheets} = \frac{1}{2}\int_A \left[\rho_1 h_1 \left(\left(\frac{\partial u_1}{\partial t} \right)^2 + \left(\frac{\partial v_1}{\partial t} \right)^2 \right) + \rho_3 h_3 \left(\left(\frac{\partial u_3}{\partial t} \right)^2 + \left(\frac{\partial v_3}{\partial t} \right)^2 \right) \right] dx\ dy \tag{12}$$

2. Kinetic energy corresponding to transverse displacement:

$$K_{Face\ sheets\ \&\ ER\ core} = \frac{1}{2}\int_A \left[\rho_1 h_1 + \rho_2 h_2 + \rho_3 h_3 \right] \left(\frac{\partial w}{\partial t} \right)^2 dx\ dy \tag{13}$$

3. Kinetic energy corresponding with the rotation of electro-rheological layer:

$$K_{ER\ core} = \frac{1}{2}\int_A I_2 \left[\left(\frac{\partial \gamma_{xz\,2}}{\partial t} \right)^2 + \left(\frac{\partial \gamma_{yz\,2}}{\partial t} \right)^2 \right] dx\ dy \tag{14}$$

5 MODELING OF ER FLUID PROPERTIES

The complex shear modulus (G^*) is provided because the Bingham plastic model does not mostly present the detailed and accurate definition of the behavior of electro-rheological materials. Complex shear modulus is divided into two parts real and imaginary. For ER materials, this property is dependent on the external electric field [35-36]. The function of the electric field has been provided by different researchers:

In the model do the quadratic function of the electric field is the only real part and the imaginary part is constant [25].

$$G = G' + iG'' \rightarrow \begin{cases} G' \approx 15000E^2 \\ G'' \approx 6900 \end{cases} \tag{15}$$

Both real and imaginary parts are a function of electric field, with the difference that the real is linear function and image is nonlinear [37].

$$G = G' + iG'' \rightarrow \begin{cases} G' \approx 50000E^2 \\ G'' \approx 2600E + 1700 \end{cases} \tag{16}$$

In this research, two above models are used and discussed.

6 EQUATIONS OF MOTION

Hamilton's principle is employed to obtain the equations of motion. The principle can be stated in an analytical form where the first variation form of equations must be zero, as follows [34]:

$$\delta \int_{t_1}^{t_2} \left[U_{Sandwich} - K_{Sandwich} \right] dt = 0 \tag{17}$$

where $\delta U_{Sandwich}$ and $\delta K_{Sandwich}$ are the variation of strain energy and variation of Kinetic energy. Substituting Eqs. (11) to (14) into Eq. (17) using dimensionless parameters which introduced in Eq. (18):

$$(\zeta,\eta)=\left(\frac{x}{a},\frac{y}{b}\right),\quad (U_i,V_i,W)=\left(\frac{u_i}{a},\frac{v_i}{b},\frac{w}{h_2}\right),\quad (\alpha_i,\beta_i)=\left(\frac{h_i}{a},\frac{h_i}{b}\right),\quad \gamma=\frac{a}{b},\quad \bar{Q}_{ij}=\frac{Q_{ij}}{Q_{11}},\quad \bar{G}=\frac{G_2}{Q_{11}},\quad \in=\frac{h_3}{h_2},\quad \delta=\frac{h_1}{h_2},$$
$$\bar{\rho}=\frac{\rho_2}{\rho_{lor3}}=\frac{\rho_E}{\rho_m},\quad K_{bw}=\frac{k_w(2h_m+h_c)}{E_m},\quad g_{xa}=\frac{g_x}{a.E_m},\quad g_{xb}=\frac{g_x}{b.E_m}=\gamma g_{xa},\quad g_{ya}=\frac{g_y}{a.E_m},\quad g_{yb}=\frac{g_y}{b.E_m}=\gamma g_{ya},\quad \lambda=\frac{g_{xa}}{g_{ya}},\tag{18}$$
$$G_{ij}=\frac{e_{ij}K_{vfc}}{\sqrt{E_mQ_{11}}},\quad \tau=\frac{t}{a}\sqrt{\frac{Q_{11}}{\rho_m}},\quad \bar{I}_i=\frac{I_i}{h_i^3}\ .$$

Setting the coefficient $\delta W,\delta V_3,\delta V_1,\delta U_3,\delta U_1$ equal to zero, the equations of motion are obtained as follows:

δU_1 :

$$\begin{aligned}&2\alpha_2\bar{G}\frac{d}{d\zeta}W-2\bar{G}/\alpha_2U_3+2\bar{G}/\alpha_2U_1+\bar{G}\delta\alpha_2\frac{d}{d\zeta}W+\bar{G}\in\alpha_2\frac{d}{d\zeta}W-\alpha_1\frac{d^2}{d\zeta^2}U_1\\&-1/2\bar{Q}_{12}\alpha_1\frac{d^2}{d\eta d\zeta}V_1+1/2S_{31}\alpha_1\alpha_2\frac{d^2}{d\tau d\zeta}W-1/2\bar{Q}_{21}\alpha_1\frac{d^2}{d\eta d\zeta}V_1+1/2\bar{\rho}\bar{I}_2\alpha_2{}^2\alpha_3\frac{d^3}{d\tau^2d\zeta}W\\&+1/2\bar{\rho}\bar{I}_2\alpha_2{}^2\alpha_1\frac{d^3}{d\tau^2d\zeta}W+\bar{\rho}\bar{I}_2\alpha_2{}^3\frac{d^3}{d\tau^2d\zeta}W+\alpha_1\frac{d^2}{d\tau^2}U_1+\bar{Q}_{44}\alpha_1\frac{d^2}{d\eta d\zeta}V_1-\bar{Q}_{44}\gamma\beta_1\frac{d^2}{d\eta^2}U_1=0\end{aligned}\tag{19}$$

δV_1 :

$$\begin{aligned}&2\bar{G}\beta_2\frac{d}{d\eta}W-2\frac{\bar{G}}{\beta_2}V_3+\beta_2\in Gb\frac{d}{d\eta}W+2\frac{\bar{G}}{\beta_2}V_1+\delta\beta_2\bar{G}\frac{d}{d\eta}W-\bar{Q}_{12}\beta_1\frac{d^2}{d\eta\mathrm{d}\zeta}U_1-\bar{Q}_{22}\beta_1\frac{d^2}{d\eta^2}V_1\\&+1/2S_{32}\beta_1\alpha_2\frac{d^2}{d\tau\mathrm{d}\eta}W+1/2\bar{\rho}\bar{I}_2\alpha_2{}^2\beta_1\frac{d^3}{d\tau^2d\eta}W+1/2\bar{\rho}\bar{I}_2\alpha_2{}^2\beta_3\frac{d^3}{d\tau^2d\eta}W+\bar{\rho}\bar{I}_2\alpha_2{}^2\beta_2\frac{d^3}{d\tau^2d\eta}W\\&-\frac{\bar{\rho}\bar{I}_2\alpha_2}{\gamma}\frac{d^2}{d\tau^2}V_3+\frac{\bar{\rho}\bar{I}_2\alpha_2}{\gamma}\frac{d^2}{d\tau^2}V_1+\frac{\alpha_1}{\gamma}\frac{d^2}{d\tau^2}V_1-\frac{\bar{Q}_{44}\alpha_1}{\gamma}\frac{d^2}{d\zeta^2}V_1-\bar{Q}_{44}\beta_1\frac{d^2}{d\zeta^2}U_1=0\end{aligned}\tag{20}$$

δU_3 :

$$\begin{aligned}&-2\alpha_2\bar{G}\frac{d}{d\zeta}W-\frac{2\bar{G}U_1}{\alpha_2}+\frac{2\bar{G}U_3}{\alpha_2}-\bar{G}\in\alpha_2\frac{d}{d\zeta}W-\bar{G}\delta\alpha_2\frac{d}{d\zeta}W-\alpha_3\frac{d^2}{d\zeta^2}U_1\\&-1/2\bar{Q}_{12}\alpha_3\frac{d^2}{d\eta\mathrm{d}\zeta}V_3+1/2S_{31}\alpha_3\alpha_2\frac{d^2}{d\tau\mathrm{d}\zeta}W-1/2\bar{Q}_{21}\alpha_3\frac{d^2}{d\eta\mathrm{d}\zeta}V_3-1/2\bar{\rho}\bar{I}_2\alpha_2{}^2\alpha_1\frac{d^3}{d\tau^2d\zeta}W\\&-1/2\bar{\rho}\bar{I}_2\alpha_2{}^2\alpha_3\frac{d^3}{d\tau^2d\zeta}W-\bar{\rho}\bar{I}_2\alpha_2{}^3\frac{d^3}{d\tau^2d\zeta}W+\alpha_3\frac{d^2}{d\tau^2}U_1-\bar{Q}_{44}\alpha_3\frac{d^2}{d\eta d\zeta}V_3-\bar{Q}_{44}\gamma\beta_3\frac{d^2}{d\eta^2}U_3=0\end{aligned}\tag{21}$$

δV_3 :

$$\begin{aligned}&-2\frac{\bar{G}}{\beta_2}V_1-2\bar{G}\beta_2\frac{d}{d\eta}W-\beta_2\in\bar{G}\frac{d}{d\eta}W-\delta\beta_2\bar{G}\frac{d}{d\eta}W+2\frac{\bar{G}}{\beta_2}V_3-1/2\bar{Q}_{12}\beta_3\frac{d^2}{d\eta\mathrm{d}\zeta}U_3-1/2\bar{Q}_{21}\beta_3\frac{d^2}{d\eta\mathrm{d}\zeta}U_3\\&-\bar{Q}_{22}\beta_3\frac{d^2}{d\eta^2}V_3+1/2S_{32}\beta_3\alpha_2\frac{d^2}{d\tau\mathrm{d}\eta}W-1/2\bar{\rho}\bar{I}_2\alpha_2{}^2\beta_1\frac{d^3}{d\tau^2d\eta}W-1/2\bar{\rho}\bar{I}_2\alpha_2{}^2\beta_3\frac{d^3}{d\tau^2d\eta}W\\&-\bar{\rho}\bar{I}_2\alpha_2{}^2\beta_2\frac{d^3}{d\tau^2d\eta}W-\frac{\bar{\rho}\bar{I}_2\alpha_2}{\gamma}\frac{d^2}{d\tau^2}V_1+\frac{\bar{\rho}\bar{I}_2\alpha_2}{\gamma}\frac{d^2}{d\tau^2}V_3+\frac{\alpha_3}{\gamma}\frac{d^2}{d\tau^2}V_3-\frac{\bar{Q}_{44}\alpha_3}{\gamma}\frac{d^2}{d\zeta^2}V_3-\bar{Q}_{44}\beta_3\frac{d^2}{d\zeta^2}U_3=0\end{aligned}\tag{22}$$

δW :

$$\begin{aligned}&-2\bar{G}\beta_2{}^2\frac{d^2}{d\eta^2}W+\alpha_2{}^2\bar{\rho}\frac{d^2}{d\tau^2}W-2\bar{G}\alpha_2{}^2\frac{d^2}{d\zeta^2}W+\alpha_2\alpha_1\frac{d^2}{d\tau^2}W+\alpha_2\alpha_3\frac{d^2}{d\tau^2}W\\&+\bar{I}_3\alpha_2\alpha_3{}^3\frac{d^4}{d\zeta^4}W+\bar{I}_1\alpha_1{}^3\alpha_2\frac{d^4}{d\zeta^4}W-2\bar{G}\beta_2\beta_3\frac{d^2}{d\eta^2}W-2\bar{G}\alpha_2\alpha_3\frac{d^2}{d\zeta^2}W-2\bar{G}\beta_2\beta_1\frac{d^2}{d\eta^2}W\\&-2\bar{G}\alpha_2\alpha_1\frac{d^2}{d\zeta^2}W-\bar{\rho}\bar{I}_2\alpha_2{}^4\frac{d^4}{d\tau^2d\zeta^2}W-\bar{\rho}\bar{I}_2\alpha_2{}^2\frac{d^3}{d\tau^2d\eta}V_1+\bar{\rho}\bar{I}_2\alpha_2{}^2\frac{d^3}{d\tau^2d\eta}V_3\end{aligned}\tag{23}$$

$$
\begin{aligned}
&+1/2\bar{\rho}\bar{I}_2\alpha_2\alpha_1\frac{d^3}{d\tau^2 d\eta}V_3+1/2\bar{\rho}\bar{I}_2\alpha_2\alpha_3\frac{d^3}{d\tau^2 d\eta}V_3-1/2\bar{\rho}\bar{I}_2\alpha_2\alpha_1\frac{d^3}{d\tau^2 d\eta}V_1-1/2\bar{\rho}\bar{I}_2\alpha_2\alpha_3\frac{d^3}{d\tau^2 d\eta}V_1\\
&-2\bar{G}\frac{d}{d\eta}V_1+2\bar{G}\frac{d}{d\eta}V_3+\bar{I}_1\bar{Q}_{21}\alpha_1^{\,2}\beta_1\beta_2\frac{d^4}{d\eta^2 d\zeta^2}W+\bar{I}_1\bar{Q}_{12}\alpha_1^{\,2}\beta_1\beta_2\frac{d^4}{d\eta^2 d\zeta^2}W+\bar{I}_3\bar{Q}_{12}\alpha_3^{\,2}\beta_3\beta_2\frac{d^4}{d\eta^2 d\zeta^2}W\\
&+\bar{I}_3\bar{Q}_{21}\alpha_3^{\,2}\beta_3\beta_2\frac{d^4}{d\eta^2 d\zeta^2}W-1/2\bar{\rho}\bar{I}_2\alpha_2^{\,2}\alpha_3\alpha_1\frac{d^4}{d\tau^2 d\zeta^2}W-1/2\bar{\rho}\bar{I}_2\alpha_2^{\,2}\beta_3\beta_1\frac{d^4}{d\tau^2 d\eta^2}W\\
&-\bar{\rho}\bar{I}_2\alpha_2^{\,2}\beta_2^{\,2}\delta\frac{d^4}{d\tau^2 d\eta^2}W-\bar{\rho}\bar{I}_2\alpha_2^{\,2}\beta_2^{\,2}\epsilon\frac{d^4}{d\tau^2 d\eta^2}W-1/4\bar{\rho}\bar{I}_2\alpha_2^{\,2}\beta_2^{\,2}\delta^2\frac{d^4}{d\tau^2 d\eta^2}W\\
&-1/4\bar{\rho}\bar{I}_2\alpha_2^{\,2}\beta_2^{\,2}\in^2\frac{d^4}{d\tau^2 d\eta^2}W-\bar{\rho}\bar{I}_2\alpha_2^{\,4}\in\frac{d^4}{d\tau^2 d\zeta^2}W-1/4\bar{\rho}\bar{I}_2\alpha_2\alpha_3^{\,3}\frac{d^4}{d\tau^2 d\zeta^2}W\\
&-1/4\bar{\rho}\bar{I}_2\alpha_2^{\,2}\alpha_1^{\,2}\frac{d^4}{d\tau^2 d\zeta^2}W-1/2\bar{G}\in\beta_2\beta_3\frac{d^2}{d\eta^2}W-\bar{\rho}\bar{I}_2\alpha_2^{\,3}\alpha_1\frac{d^4}{d\tau^2 d\zeta^2}W\\
&-\bar{\rho}\bar{I}_2\alpha_2^{\,2}\beta_2^{\,2}\frac{d^4}{d\tau^2 d\eta^2}W-1/2\bar{G}\delta\alpha_1\alpha_2\frac{d^2}{d\zeta^2}W-1/2\bar{G}\delta\beta_1\beta_2\frac{d^2}{d\eta^2}W\\
&-\bar{G}\delta\beta_2\beta_3\frac{d^2}{d\eta^2}W-\bar{G}\delta\alpha_2\alpha_3\frac{d^2}{d\zeta^2}W-1/2\bar{G}\in\alpha_2\alpha_3\frac{d^2}{d\zeta^2}W+\bar{I}_3\bar{Q}_{22}\beta_3^{\,3}\beta_2\frac{d^4}{d\eta^4}W\\
&+\bar{I}_1\bar{Q}_{22}\alpha_1^{\,3}\alpha_2\frac{d^4}{d\eta^4}W+1/2\alpha_1 S_{32}\frac{d^2}{d\tau\mathrm{d}\eta}V_1-\bar{G}\in\frac{d}{d\eta}V_1-\bar{G}\delta\frac{d}{d\eta}V_1+\bar{G}\in\frac{d}{d\eta}V_3\\
&+1/2S_{32}\beta_3\frac{d^2}{d\tau\mathrm{d}\eta}V_3+\bar{G}\delta\frac{d}{d\eta}V_3+4\bar{I}_1\bar{Q}_{44}\alpha_1^{\,2}\beta_1\beta_2\frac{d^4}{d\eta^2 d\zeta^2}W+4\bar{I}_3\bar{Q}_{44}\alpha_3^{\,2}\beta_1\beta_2\frac{d^4}{d\eta^2 d\zeta^2}W\\
&+1/2\bar{\rho}\bar{I}_2\alpha_2\alpha_1\frac{d^3}{d\tau^2 d\zeta}U_3+1/2\bar{\rho}\bar{I}_2\alpha_2\alpha_3\frac{d^3}{d\tau^2 d\zeta}U_3+\bar{\rho}\bar{I}_2\alpha_2^2\frac{d^3}{d\tau^2 d\zeta}U_3+2\bar{G}\frac{d}{d\zeta}U_3\\
&+\bar{G}\in\frac{d}{d\zeta}U_3+\bar{G}\delta\frac{d}{d\zeta}U_3+1/2\beta_3 S_{31}\frac{d^2}{d\tau\mathrm{d}\zeta}U_3-1/2\bar{\rho}\bar{I}_2\alpha_2\alpha_1\frac{d^3}{d\tau^2 d\zeta}U_1-1/2\bar{\rho}\bar{I}_2\alpha_2\alpha_3\frac{d^3}{d\tau^2 d\zeta}U_1\\
&-\bar{\rho}\bar{I}_2\alpha_2^2\frac{d^3}{d\tau^2 d\zeta}U_1-2\bar{G}\frac{d}{d\zeta}U_1-\bar{G}\in\frac{d}{d\zeta}U_1-\bar{G}\delta\frac{d}{d\zeta}U_1+1/2\alpha_1 S_{31}\frac{d^2}{d\tau\mathrm{d}\zeta}U_1=0
\end{aligned}
\tag{23}
$$

where $Ii=\int_{h_c/2}^{(h_c/2+h_m)} z^i\,dz+\int_{-(h_c/2+h_m)}^{-h_c/2} z^i\,dz,\quad (i=2,4,6)$.

7 SOLUTION PROCEDURE USING DQM

At first Eq. (19) is used for separation of variables in space and time distribution:

$$
\begin{aligned}
&U_1(\zeta,\eta,\tau)=U_1(\zeta,\eta)\;e^{\omega\tau},\\
&U_3(\zeta,\eta,\tau)=U_3(\zeta,\eta)\;e^{\omega\tau},\\
&V_1(\zeta,\eta,\tau)=V_1(\zeta,\eta)\;e^{\omega\tau},\\
&V_3(\zeta,\eta,\tau)=V_3(\zeta,\eta)\;e^{\omega\tau},\\
&W(\zeta,\eta,\tau)=W(\zeta,\eta)\;e^{\omega\tau},
\end{aligned}
\tag{24}
$$

where $\omega=\Omega a\sqrt{\rho_m/E_m}$ is the dimensionless frequency (Ω is the dimensional frequency). DQM can change the differential equations into the first algebraic equations. In this regard, the partial derivatives of a function (F) are approximated by a specific variable, at discontinuous points by a set of weighting series. It's supposed that F be a function representing U,V,W,θ_1 and θ_2 with respect to variables ξ and η ($0<\xi<1, 0<\eta<1$) when $N_\xi\times N_\eta$ be the grid points along these variables with following derivative [38]:

$$\frac{d^n F(\xi_i,\eta_j)}{d\xi^n}=\sum_{k=1}^{N_\xi}A_{ik}^{(n)}F(\xi_k,\eta_j) \qquad n=1,...,N_\xi-1,$$
$$\frac{d^m F(\xi_i,\eta_j)}{d\eta^m}=\sum_{l=1}^{N_\eta}B_{jl}^{(m)}F(\xi_i,\eta_l) \qquad m=1,...,N_\eta-1, \tag{25}$$
$$\frac{d^{n+m} F(\xi_i,\eta_j)}{d\xi^n d\eta^m}=\sum_{k=1}^{N_\xi}\sum_{l=1}^{N_\eta}A_{ik}^{(n)}B_{jl}^{(m)}F(\xi_k,\eta_l)$$

where $A_{ik}^{(n)}$ and $B_{jl}^{(m)}$ are the weighting coefficients using Chebyshev polynomials for the positions of the grid points whose recursive formulae can be found in [38]. Applying DQM and using Eq. (20) into governing Eqs. (19), the standard form of vibrational motion equation set $(M\partial^2X/\partial t^2+C\partial X/\partial t+KX=0)$ is obtained and by considering simply supported boundary conditions an eigenvalue problem is derived in which the eigen-values of the state-space matrix $\left([\text{state}-\text{space}]=\begin{bmatrix}[0] & [\text{I}]\\ -[\text{M}^{-1}\text{K}] & -[\text{M}^{-1}\text{C}]\end{bmatrix}\right)$ are the dimensionless frequency. It is worth to mention that M is the mass matrix, C is the damping matrix and K is the stiffness, $[I]$ and $[0]$ are the unitary and zero matrixes.

8 NUMERICAL RESULTS AND DISCUSSION

The present research investigated the free vibration of the sandwich plate when the plate composed of magnetostrictive face sheets and ER fluid. The sandwich core was filled with ER fluid, and the top and bottom layers of the sandwich were made of Ms materials and the three layers vibrated as a single sandwich. The ER fluid was placed into a uniform magnetic field controlled by a vibration frequency feedback system. Then the frequency response of sandwich plate was evaluated using velocity feedback gain, aspect ratio, core-to-face sheet thickness ratio, thickness ratio. The mechanical properties of Terfenol-D as face sheet are listed at Table 1.

Density and Poisson's ratio of ER fluid are assumed to be $\rho=1700(kg/m^3)$ and $\upsilon=0.3$ [25]. Electric field is changed between $0.2\le E_*(kV/mm)\le 3.5$ because ER fluid works in the especial range of electric field due to inherit properties.

Table 1
Material properties of face sheet (Terfnol D) [22,32,33].

Properties	E	υ	ρ	$e_{31}=e_{32}$
Terfenol-D	$30\times10^9\,Pa$	0.25	$9.25\times10^3\,kg/m^3$	$442.55N/(m.A)$

This paper investigates the vibration of a sandwich plate with a constraining layer (the materials of the constrained layer is aluminum) and an ER fluid core. Fig. 4 compares the results of the present work by Yeh and Chen [30]. Fig. 5 shows the variation of dimensionless frequency versus core to face sheet thickness. For this purpose, ten points with different thickness ratios in Fig. 6 of Yeh and Chen [30] are compared with DQM solution by using Getdata software Most of the error is related to the endpoint and it is approximately equal to 0.07. As can be seen from the figure, there is a good agreement among the results of present work and Yeh and Chen [30].

Figs. 5 to 17 show the dimensionless frequency changes of the sandwich plate relative to the applied electric field for various parameters.

Loss factor: According to studies, Bingham plastic model provides the most detailed and accurate definition of the behavior of electro-rheological materials to design. In this regard, the complex shear modulus is introduced to predict the behavior of these materials.

Complex shear modulus is divided into two real and imaginary parts. The storage modulus and loss modulus are used for real and imaginary parts respectively. These properties are dependent on the external electric field for ER materials. To calculate the loss factor in an ER fluid containing system as provided in this article, the real and imaginary parts of frequency are detected and loss factor is introduced as follows:

$$If\ e^{\omega\tau} \mapsto \omega = \mathrm{Re}(\omega) + i\ \mathrm{Im}(\omega) \mapsto Loss\ factor = \frac{\mathrm{Re}(\omega)}{\mathrm{Im}(\omega)} = \frac{\xi}{\sqrt{1-\xi^2}}$$

Fig. 5 shows the changes of real and imaginary parts and the ratio between them versus the damping coefficient $(0 \le \xi \le 1)$ for the standard second order vibration system. This changes have been displayed for better understanding about loss factor. It is found from Fig. 5 when $\xi < 0.7 \mapsto 0 \le Loss\ factor < 1$ because $\xi \approx 0.7 \mapsto \xi = \sqrt{1-\zeta^2}$ and for $\xi > 0.7 \mapsto Loss\ factor > 1$.

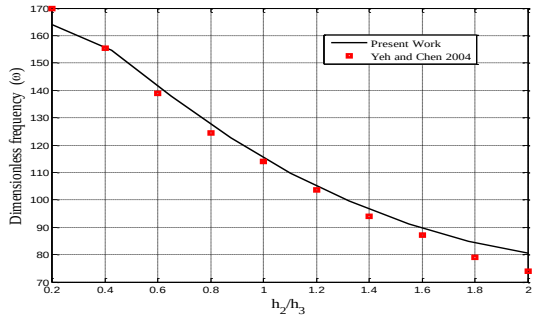

Fig.4
Comparison the results with Yeh and Chen [30].

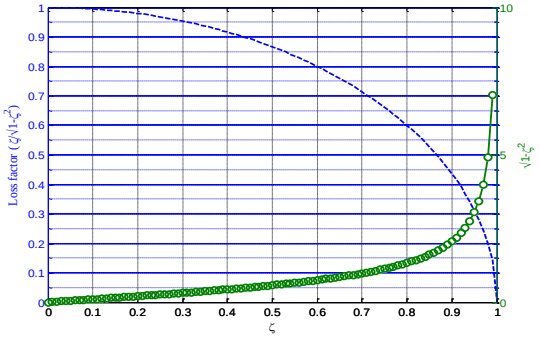

Fig.5
Display of real and imaginary part of complex frequency versus damping parameter.

Fig. 6 and 7 shows the variations of real, image and loss factor for the model(a) and (b) of the ER core with increasing the core thickness ratio. It is worth to mention that decreasing the loss factor means that the loss modulus decreases or the storage modulus increases. The stiffness of ER fluid enhanced when the loss factor drops. These results are extracted for high values of the electric field and the effect of the electric field on the face sheets has been eliminated to show more clearly the effect of the complex shear modulus on the ER core. In the model (b), the frequency is larger than the model (a) so the loss factor is greater.

If there were no damping, only the real part of the frequency was the natural frequency. In the presence of damp, the natural frequency obtains from $\omega_n = \sqrt{|complex\ \ frequency|^2}$.

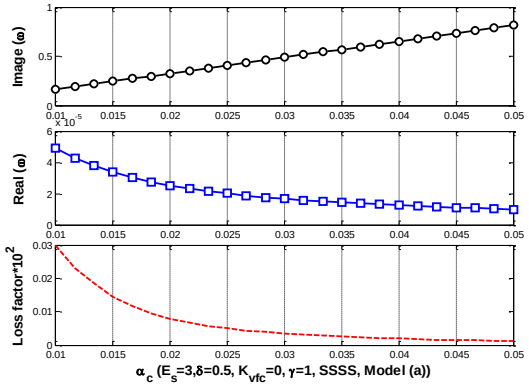

Fig.6
Variation of loss factor, real and imaginary part of complex frequency versus core thickness ratio for model (a).

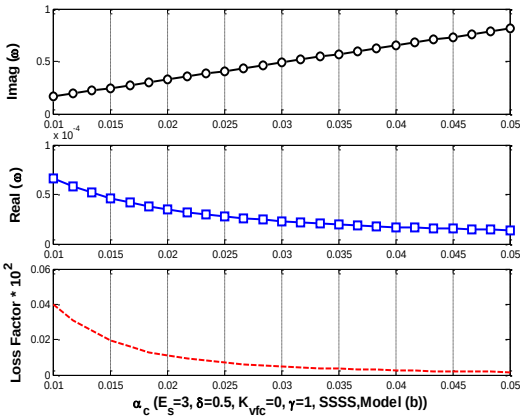

Fig.7
Variation of loss factor, real and imaginary part of complex frequency versus core thickness ratio for model (b).

Fig. 8 compares the result of Don (Model(a)) and Yalcintas (Model(b)) models. In Model(b), both real and imaginary shear modules are changed by the external electric field. Curves in two different models show that with increasing the electric field intensity, the dimensionless frequency of sandwich plate increases. Such a process is implemented with the results by other researchers in the field. Because by increasing the electric field strength, shear modulus and viscosity of the fluid are changed, so the masses in the fluid form a solid chain, and the fluid convert to the solid-like gel and ultimately increase the dimensionless frequency of sandwich plate. According to Fig. 8, it can be seen that the values of dimensionless frequency and gradient of Model(b) is more.

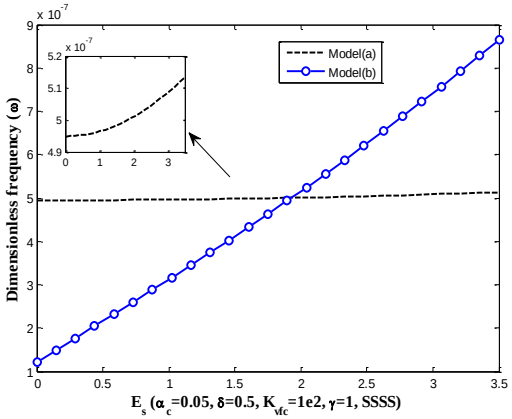

Fig.8
Variation of dimensionless frequency versus electric field for three models.

In a simple definition, the thin and flat structural element is called a plate, which is divided by the thickness ratio as follows:

Thin: $0.01 < h/a < 0.05$,

Thick: $0.05 < h/a < 0.3$,

The classical theory of plates is applicable to very thin and moderately thin plates. According to the selected theory and the assumptions presented in deriving the governing equations, the thickness of this structure should be within the range of thin plates.

Fig. 9 displays the dimensionless frequency changes of sandwich plate versus applied electric field in different thickness ratios of the core. As can be seen, the changes of dimensionless frequency versus electric field in front of their changes versus α_c are small. According to the figure, increasing the ratio of core thickness leads to decrease the frequency. An increase in this dimensionless parameter $(\alpha_c = h_2/a)$ may indicate an increase in core thickness. Therefore, the results show that as the core thickness increases, the frequency of the system decreases, in other words, this parameter decreases the stiffness of system. Since a sandwich is a structural definition whose core is thicker than the crust, this structure with a thicker core will have lower frequency. The reason for this result can be clearly attributed to the loss modulus of ER fluid.

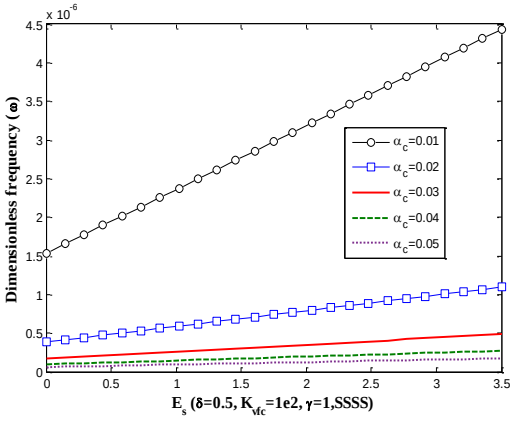

Fig.9
Variation of dimensionless frequency versus electric field in different α_c .

Fig. 10 display the dimensionless frequency changes of sandwich plate versus applied electric field in different δ . According to the definition of $\delta = h_m / h_c$ increasing the thickness of ER core reduces δ and the figure displays the non-dimensional frequency of sandwich plate increases by decreasing δ . In other words, the same result was derived from the previous figure. If the thickness of the core remains constant or its variation is small as the Ms face sheets thickness increases, the results show that the frequency decreases. Fig. 11 is a three dimensional representation of dimensionless frequency versus α_c , δ at the same time. Delta variations are greater in thinner plates and the lowest frequency of the structure is where the thickness of the face sheets and the core are equal and $\alpha_c = 0.05$ .This is while the maximum of frequency occurs in $\alpha_c = 0.01$, $\delta = 0.25$ where both values are minimal.

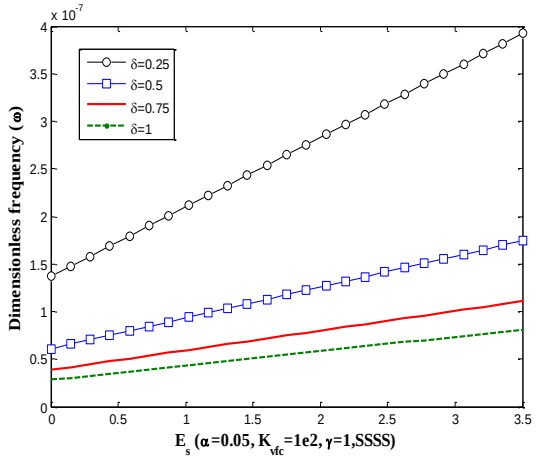

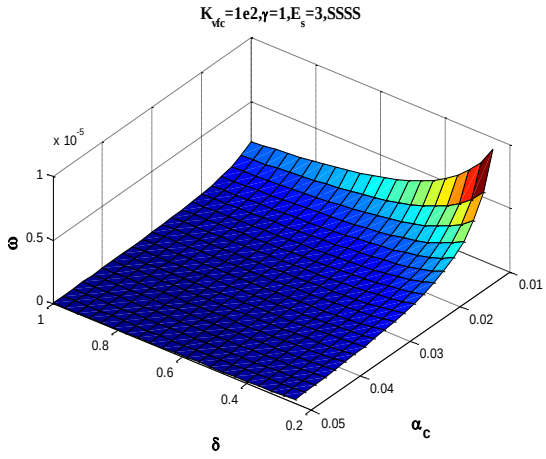

Fig.10
Variation of dimensionless frequency versus electric field in different δ .

Fig.11
3D plot of dimensionless frequency versus α_c , δ .

Fig. 12 also is a three dimensional representation of dimensionless frequency versus α_c, γ at the same time. Two Figs. 11 and 12 show the frequency changes of the structure with changes in the geometry of sandwich plate. The most important points in these three-dimensional figures are the maximum and the minimum. Variations of γ are greater in thinner plates and the lowest frequency of the structure is for rectangular plate where $\alpha_c = 0.05$ .This is while the maximum of frequency occurs in maximum of γ and minimum of α_c .

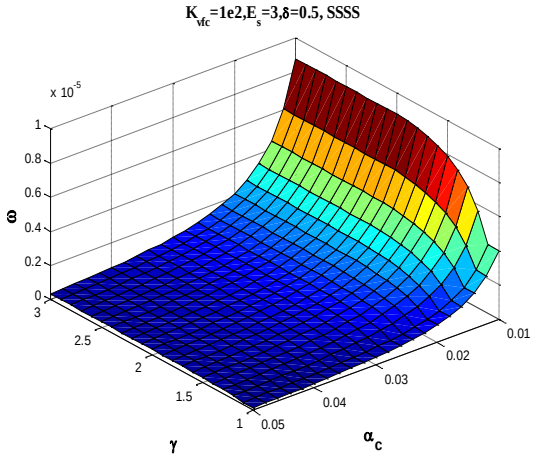

Fig.12
3D plot of dimensionless frequency versus α_c, γ .

It should be noted when the MsMs is exposed to magnetic field, they deform due to reciprocal nature. By changing in velocity feedback gain parameter K_{vfc} can be controlled the MsP frequency. In MsM, the applied magnetic field causes changes in the stress relations. Such a physical reaction is called magneto-mechanical coupling and can be used to stabilize the mechanical system containing MsM. In this study, a feedback control system was used which is able to modify the frequency response of the system by magneto-mechanical coupling.

Figs. 13 and 14 display the dimensionless frequency changes of sandwich plate versus applied electric field in different velocity feedback control parameter. There is an increase in this parameter (K_{vfc}), the dimensionless frequency is reduced in both figures, the same result is already expected. It was mentioned earlier that this parameter represents the intensity of the applied magnetic field on magnetostrictive face sheets of sandwich plate. Increasing the velocity feedback control parameter reduces the frequency at all values of the electric field applied to the ER core that it can be used to absorb vibration or canceled. Fig.13 is three-dimensional plot and Fig.14 is two-dimensionless of changes in E_s ,K_{vfc} . The intelligentness of the structure can be recognized by these two figures. Electric field changes the vibrational behavior of ER fluid and the magnetic field affects the sandwich Ms face sheets. In fact, the vibrational properties of the structure can be changed by means of electric and magnetic fields.

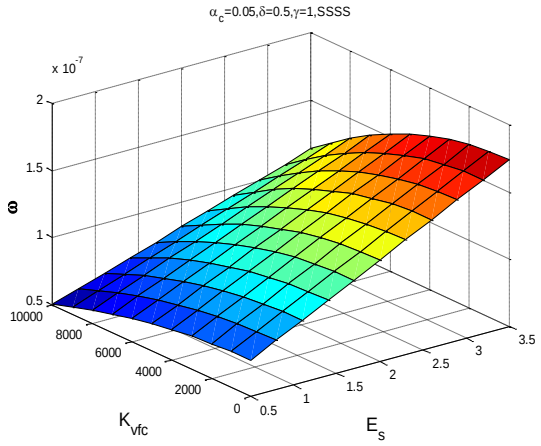

Fig.13
3D plot of dimensionless frequency versus K_{vfc}, E_s .

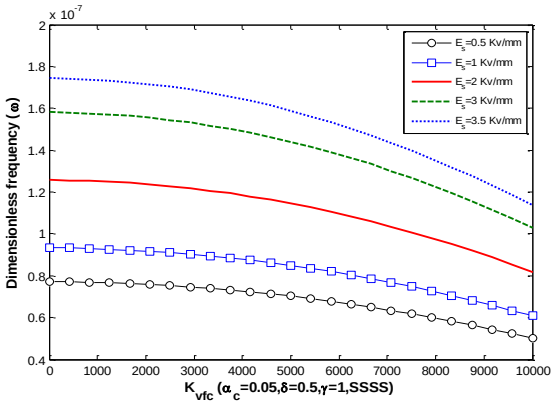

Fig.14
2D plot of dimensionless frequency versus K_{vfc} in different electric fields.

Fig. 15 shows that the amplification of velocity feedback control increases the loss factor. Based on the evidence and findings that were taken in earlier Figs, by increasing the velocity feedback control parameters and subsequently changing the behavior of Ms facesheets, the dimensionless frequency of sandwich plate falls and at the same time loss factor increases. In fact, by gain of feedback control, the magnetic field intensity can be increased, in which case the system frequency drops and the loss factor subsequently increases.

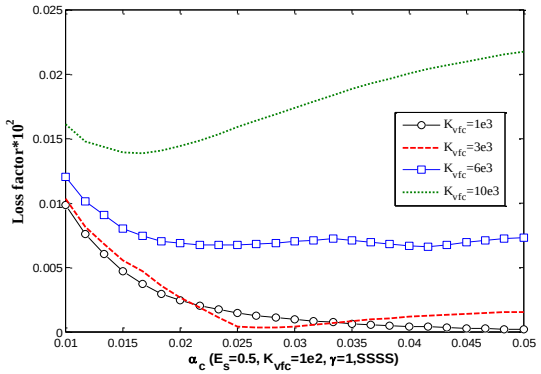

Fig.15
Variation of loss factor versus α_c in different K_{vfc} .

All of the figures were plotted for simply supported boundary condition but figure 16 displays the effect of different boundary condition. It can be seen that the frequencies of the clamped conditions due to more rigidity than simply supported condition, are more. On the other, the changes rate of the frequency is bigger in thin plate.

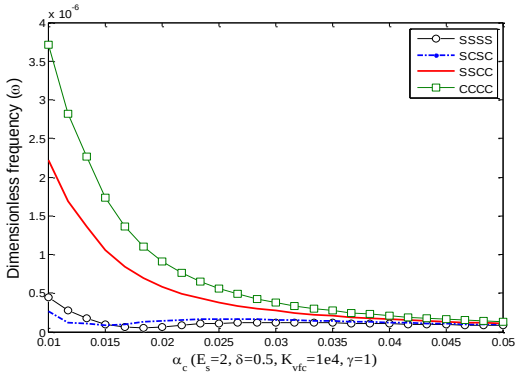

Fig.16
Variation of dimensionless frequency versus α_c for different boundary conditions.

9 CONCLUSIONS

Free vibration of the sandwich plate with electro-rheological core and magnetostrictive face sheet is a novel topic that has been studied in this research for the first time. To consider the magnetization effect of face sheet, a control

feedback system was used and velocity feedback gain as controlling parameter was introduced. Using Bingham plastic model, the complex shear modulus is presented for electro-rheological fluid based on Don (Model(a)) and Yalcintas (Model(b)) models. Using plat theory, the governing equations were derived and two dimensional DQM was utilized to solve them, findings show:

- Increasing of electric field strength changes the shear modulus and viscosity of the fluid (the fluid convert to the solid-like gel) and subsequently increases the dimensionless frequency of sandwich plate.
- The frequency decreases when the ratio of core thickness decreases. The thicker the ER core, the lower the frequency of the structure due to loss modulus.
- Increasing the aspect ratio leads to increase the frequency. In the given interval and in the same conditions, the lowest frequency for this structure belongs to square geometry.
- Increasing the electric field and subsequently changing the nature of the ERl fluid to solid-like gel, the dimensionless frequency of sandwich plate is increased and at the same time loss factor fall.
- The rate of changes in Yalcintas model ($Model(b)$) was faster than Don model ($Model(a)$).
- The frequency of the vibrating system can be changed by the gain of control in the feedback control system with changes in the magnitude of the applied magnetic field. Such a feature can help engineers to design a variety of controllers for such systems.

Since the electric field increases the damping effect, ER materials can be used to enhance system stability.

REFERENCES

[1] Jalili N., 2010, *Piezoelectric-Based Vibration Control: From Macro to Micro/Nano Scale Systems*, Springer, New York, US.

[2] Mikhasev G.I., Altenbach H., Korchevskaya E.A., 2014, On the influence of the magnetic field on the eigenmodes of thin laminated cylindrical shells containing magnetorheological elastomer, *Composite Structures* **113**(1):186-196.

[3] Arumugam A.B., Ramamoorthy M., Rajamohan V., Mageshwaran S., Rajesh Kumar S., 2018, Dynamic characterization and parametric instability analysis of rotating magnetorheological fluid composite sandwich plate subjected to periodic in-plane loading, *Journal of Sandwich Structures & Materials* **21**(6): 2099-2126.

[4] Malekzadeh Fard K., Gholami M., Reshadi F., livani M., 2017, Free vibration and buckling analyses of cylindrical sandwich panel with magneto rheological fluid layer, *Journal of Sandwich Structures & Materials* **19**(4): 397-423.

[5] Sainsbury M.G., Zhang Q.J., 1997, The Galerkin element method applied to the vibration of damped sandwich beams, *Computers & Structures* **71**(3): 239-256.

[6] Yeh J.Y., Chen L.W., 2005, Dynamic stability of a sandwich plate with a constraining layer and electrorheological fluid core, *Journal of Sound and Vibration* **285**(3): 637-652.

[7] Lu H., Guang M., 2006, An experimental and analytical investigation of the dynamic characteristics of a flexible sandwich plate filled with electrorheological fluid, *International Journal of Advanced Manufacturing Technology* **28**(11-12): 1049-1055.

[8] Yeh J.Y., Chen L.W., 2006, Dynamic stability analysis of a rectangular orthotropic sandwich plate with an electrorheological fluid core, *Composite Structures* **72**(1): 33-41.

[9] Narayana G.V., Ganesan N., 2007, Critical comparison of viscoelastic damping and electrorheological fluid core damping in composite sandwich skew plates, *Composite Structures* **80**(2): 221-233.

[10] Yeh J.Y., Chen L.W., 2007, Finite element dynamic analysis of orthotropic sandwich plates with an electrorheological fluid core layer, *Composite Structures* **78**(3): 368-376.

[11] Yeh J.Y., 2007, Vibration analyses of the annular plate with electrorheological fluid damping treatment, *Finite Elements in Analysis and Design* **43**(11-12): 965-974.

[12] Allahverdizadeh A., Mahjoob M.J., Eshraghi I., Nasrollahzadeh N., 2013, On the vibration behavior of functionally graded electrorheological sandwich beams, *International Journal of Mechanical Science* **70**: 130-139.

[13] Tabassian R., Rezaeepazhand J., 2013, Dynamic stability of smart sandwich beams with electro-rheological core resting on elastic foundation, *Journal of Sandwich Structures and Materials* **15**(1): 25-44.

[14] Hoseinzadeh M., Rezaeepazhand J., 2014, Vibration suppression of composite plates using smart electrorheological dampers, *International Journal of Mechanical Sciences* **84**: 31-40.

[15] Soleymani M.M., Hajabasi M.A., Elahi Mahani S., 2016, Free vibrations analysis of a sandwich rectangular plate with electrorheological fluid core, *JCARME* **5**(1): 71-81.

[16] Eshaghi M., Sedaghati R., Rakheja S., 2015, Dynamic characteristics and control of magnetorheological/electrorheological sandwich structures: A state-of-the-art review, *Journal of Intelligent Material Systems and Structures* **27**(15): 2003-2037.

[17] Hasheminejad S.M., Motaaleghi M.A., 2015, Aeroelastic analysis and active flutter suppression of an electro-rheological sandwich cylindrical panel under yawed supersonic flow, *Aerospace Science and Technology* **42**: 118-127.

[18] Asgari M., Kouchakzadeh M.A., 2016, Aeroelastic characteristics of magneto-rheological fluid sandwich beams in supersonic airflow, *Composite Structures* **143**: 93-102.
[19] Eshaghi M., Sedaghati R., Rakheja S., 2016, Analytical and experimental free vibration analysis of multi-layer MR-fluid circular plates under varying magnetic flux, *Composite Structures* **157**: 78-86.
[20] Ghorbanpour Arani A., Jamali S.A., BabaAkbar Zarei H., 2017, Differential quadrature method for vibration analysis of electro-rheological sandwich plate with CNT reinforced nanocomposite facesheets subjected to electric field, *Composite Structures* **180**: 211-220.
[21] Lee S.J., Reddy J.N., Rostam-Abadi F., 2004, Transient analysis of laminated composite plates with embedded smart-material layers, *Finite Elements in Analysis and Design* **40**(5-6): 463-483.
[22] Hong C.C., 2010, Transient responses of magnetostrictive plates by using the GDQ method, *European Journal of Mechanics B-Fluids* **29**(6): 1015-1021.
[23] Ghorbanpour Arani A., Khoddami Maraghi Z., 2016, A feedback control system for vibration of magnetostrictive plate subjected to follower force using sinusoidal shear deformation theory, *Ain Shams Engineering Journal* **7**(1): 361-369.
[24] Ghorbanpour Arani A., Khani Arani H., Khoddami Maraghi Z., 2016, Vibration analysis of sandwich composite micro-plate under electro-magneto-mechanical loadings, *Applied Mathematical Modelling* **40**(23-24): 10596-10615.
[25] Don D.L., 1993, *An Investigation of Electrorheologial Material Adaptive Structures*, Theses and Dissertations, Lehigh University, US.
[26] Brockmann T.H., 2009, *Theory of Adaptive Fiber Composites*, Springer, Dordrecht Heidelberg, London.
[27] Yalcintas M., Coulter J.P., 1995, Analytical modeling of electrorheological material based adaptive beams, *Journal of Intelligent Material Systems and Structures* **6**(4): 488-497.
[28] Ghorbanpour Arani A., Haghparast E., Khoddami Maraghi Z., 2015, Vibration analysis of double bonded composite pipe reinforced by BNNTs conveying oil, *Journal of Computational Applied Mechanics* **46**(2): 93-105.
[29] Rezaeepazhand J., Pahlavan L., 2009, Transient response of sandwich beams with electrorheological core, *Journal of Intelligent Material Systems and Structures* **20**(2): 171-179.
[30] Yeh J.Y., Chen L.W., 2004, Vibration of a sandwich plate with a constrained layer and electrorheological fluid core, *Composite Structures* **65**(2): 251-258.
[31] Wei K., Meng G., Zhang W., Zhou S., 2007, Vibration characteristics of rotating sandwich beams filled with electrorheological fluids, *Journal of Intelligent Material Systems and Structures* **18**(11): 1165-1173.
[32] Hong C.C., 2009, Transient responses of magnetostrictive plates without shear effects, *International Journal of Engineering Science* **47**(3): 355-362.
[33] Krishna M., Anjanappa M., Wu Y.F., 1997, The use of magnetostrictive particle actuators for vibration attenuation of flexible beams, *Journal of Sound and Vibration* **206**(2): 133-149.
[34] Reddy J.N., 2000, *Energy Principles and Variational Methods in Applied Mechanics*, John Wiley and Sons Publishers Texas, US.
[35] Choi S.B., Park Y.K., Kim J.D., 1993, Vibration characteristics of hollow cantilevered beams containing an electro-rheological fluid, *International Journal of Mechanical Sciences* **35**(9): 757-768.
[36] Lee C,Y., Cheng C.C., 2000, Complex moduli of electrorheological material under oscillatory shear, *International Journal of Mechanical Sciences* **42**(3): 561-573.
[37] Yalcintas M., Coulter J.P., 1995, Electrorheological material based adaptive beams subjected to various boundary conditions, *Journal of Intelligent Material Systems and Structures* **6**(5): 700-717.
[38] Shu C., 2000, *Differential Quadrature and its Application in Engineering*, Springer Publishers, Singapore.